Characterization of a quantum phase transition in Dirac systems by means of the wave-packet dynamics

E. Romera and J. J. Torres

Citation: AIP Advances **2**, 042121 (2012); doi: 10.1063/1.4764862
View online: http://dx.doi.org/10.1063/1.4764862
View Table of Contents: http://scitation.aip.org/content/aip/journal/adva/2/4?ver=pdfcov
Published by the AIP Publishing

Articles you may be interested in

Quantum Phase Transitions in Atomic Nuclei.
AIP Conf. Proc. **1012**, 3 (2008); 10.1063/1.2939345

Quantum Phase Transitions in Finite Nuclei: Theoretical Concepts and Experimental Evidence
AIP Conf. Proc. **899**, 11 (2007); 10.1063/1.2733030

Langevin Dynamics of Chiral Phase Transition at Finite Temperature and Density
AIP Conf. Proc. **739**, 634 (2004); 10.1063/1.1843677

Criteria for PhaseTransitions in Yukawa Systems (Dusty Plasma)
AIP Conf. Proc. **649**, 471 (2002); 10.1063/1.1527826

Effect of competition between Coulomb and dispersion forces on phase transitions in ionic systems
J. Chem. Phys. **114**, 3617 (2001); 10.1063/1.1342814

All article content, except where otherwise noted, is licensed under a Creative Commons Attribution 3.0 Unported license. See: http://creativecommons.org/licenses/by/3.0/
Downloaded to IP: 150.214.23.191 On: Wed, 18 Jun 2014 09:04:25

Characterization of a quantum phase transition in Dirac systems by means of the wave-packet dynamics

E. Romera[1] and J. J. Torres[2]
[1]*Departamento de Física Atómica, Molecular y Nuclear and Instituto Carlos I de Física Teórica y Computacional, Universidad de Granada, Fuentenueva s/n, 18071 Granada, Spain*
[2]*Departamento de Electromagnetismo y Física de la Materia and Instituto Carlos I de Física Teórica y Computacional, Universidad de Granada, Fuentenueva s/n, 18071 Granada, Spain*

(Received 26 July 2012; accepted 11 October 2012; published online 23 October 2012)

We study the signatures of phase transitions in the time evolution of wave-packets by analyzing two simple model systems: a graphene quantum dot model in a magnetic field and a Dirac oscillator in a magnetic field. We have characterized the phase transitions using the autocorrelation function. Our work also reveals that the description in terms of Shannon entropy of the autocorrelation function is a clear phase transition indicator. *Copyright 2012 Author(s). This article is distributed under a Creative Commons Attribution 3.0 Unported License*. [http://dx.doi.org/10.1063/1.4764862]

I. INTRODUCTION

The temporal evolution of wave-packets, relativistic and nonrelativistic, can depict interesting phenomena due to quantum interference and several types of periodicity may appear which depend on the eigenvalue spectrum of the Hamiltonian. The Jaynes Cummings model shows this type of periodicities, in particular Rabi oscillations and collapses and revivals of these Rabi oscillations.[1] These interference quantum phenomena have been widely investigated theoretically among other in different atomic and molecular quantum systems,[1–5] and observed experimentally in, for example, Rydberg wave-packets in atoms and molecules, molecular vibrational states, and Bose-Einstein condensates,[6] to name a few. Additionally, revivals of electric currents in graphene and graphene quantum dots in the presence of a magnetic field[7] have been theoretically predicted and an exhaustive study of quantum wave-packet revivals, fractional revivals and classical periodicity was recently reported.[7–11]

In this work, we study the influence of a phase transition (PT) on the time evolution of localized wave-packets by means of the autocorrelation function. Thus, we will show that in the PT points (the critical points) an abrupt change in the dynamic of localized wave-packets around the ground state appears, which includes, as main features, the exhibition of a periodic motion around them, a change in the direction of wave-packet rotation during these oscillations above and below the critical point, and a divergence of the period of these oscillations just at the critical point. For a more clear and deep analysis of the phenomena emerging at these critical points, we will use the Shannon entropy for a visualization of the changes in the dynamic of the wave packet. In fact, Shannon entropy and others information measures have been used recently to characterize quantum phase transitions in Dicke and Vibron models.[12–16]

To address this study and to see the generality of our findings we will consider two different model systems: in Section II we will consider a circular graphene quantum dot model and in section III we will study a Dirac oscillator. They provide a simple and clear framework to study the connection between PT and wave-packet dynamics.

II. GRAPHENE QUANTUM DOT MODEL

We have investigated the appearance of phase transitions in a graphene quantum dot in a perpendicular magnetic field when the magnetic field strength **B** is changed.

 © Author(s) 2012

All article content, except where otherwise noted, is licensed under a Creative Commons Attribution 3.0 Unported license. See: http://creativecommons.org/licenses/by/3.0/
Downloaded to IP: 150.214.23.191 On: Wed, 18 Jun 2014 09:04:25

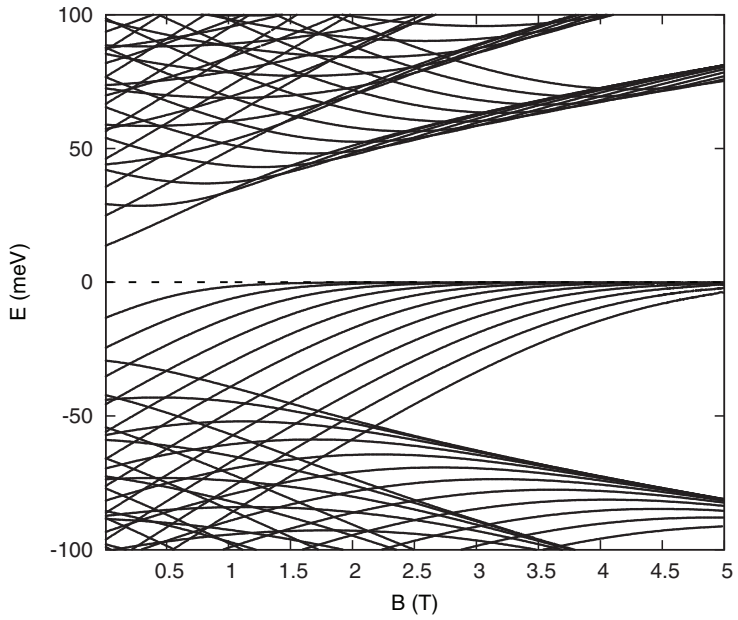

FIG. 1. Energy spectrum of an electron confined in a circular graphene quantum dot in a perpendicular magnetic field for $0\ \mathrm{T} < B < 5\ \mathrm{T}$, $\tau = 1$, $m = -11, \ldots, 7$ and energies $-100\ \mathrm{meV} \leq E \leq 100\ \mathrm{meV}$.

Graphene is a system that, in the last years, has attracted growing interest due to its remarkable and starling properties and its potential applications in nanoelectronics.[17–22] Recently, moreover, graphene quantum dots have been widely studied, both theoretically and experimentally (see[23–26] and references therein), and have been point out to be very attractive as spin qubits in quantum information processing.[25]

In the following, we will briefly describe the mathematical framework used to study graphene quantum dots. Let us consider a Hamiltonian for electrons in the valley-isotropic form by[27]

$$H_\tau = v_F(\mathbf{p} + e\mathbf{A}) \cdot \boldsymbol{\sigma} + \tau V(r)\sigma_z, \tag{1}$$

and use the symmetric gauge for the vector potential, $\mathbf{A} = B/2(-y, x, 0) = B/2(-r\sin\phi, r\cos\phi, 0)$, where ϕ is the polar angle, $v_F = 10^6 m/s$ the Fermi velocity, and $\tau = \pm 1$ differentiates the two valleys K_1 and K_2. In (1) $\boldsymbol{\sigma}$ are the Pauli spin matrices in the basis of the two sublattices of A and B atoms. On the other hand, the confinement potential is a mass-related potential energy $V(r)$ coupled to the Hamiltonian via the σ_z Pauli matrix, where $V(r) = 0$ for $r < R$ and $V(r) = \infty$ for $r > R$, that is, tends to infinity at the edge of the dot.

Upon introducing the magnetic length $l_B = \sqrt{\hbar/(eB)}$ and using the fact that H_τ commutes with the total angular momentum operator $J_z = L_z + \frac{\hbar}{2}\sigma_z$, $[H_\tau, J_z] = 0$, the solution of the Dirac equation $H_\tau\psi(r, \phi) = E\psi(r, \phi)$ (where $\psi(r, \phi) = [\psi_1(r, \phi), \psi_2(r, \phi)]$ is a two-component spinor) is given in.[27] The characteristic equation for the allowed eigenenergies E of the Quantum Dot using the boundary condition for a circular confinement[27,28] $\psi_2/\psi_1 = \tau\ \exp[i\phi]$ has been obtained in[27] and it can be written as

$$\left(1 - \tau\frac{kl_B}{R/l_B}\right) L\left(\frac{k^2l_B^2}{2} - (m+1), m, R^2/2l_B^2\right) + L\left(\frac{k^2l_B^2}{2} - (m+2), m+1, R^2/2l_B^2\right) = 0, \tag{2}$$

where $L(a, b, z)$ is the generalized Laguerre function. The spectrum of electrons confined in a circular graphene quantum dot in a perpendicular magnetic field is given by $E(n, m, \tau)$, as it is depicted in Fig. 1 for $\tau = 1$, verifying above equation and the energy eigenfunctions are $\psi_{(n,m)}(r, \phi)$. On the other hand, for $\tau = -1$ it can be taken into account that $E(n, m, 1) = -E(n, m, -1)$.

All article content, except where otherwise noted, is licensed under a Creative Commons Attribution 3.0 Unported license. See: http://creativecommons.org/licenses/by/3.0/
Downloaded to IP: 150.214.23.191 On: Wed, 18 Jun 2014 09:04:25

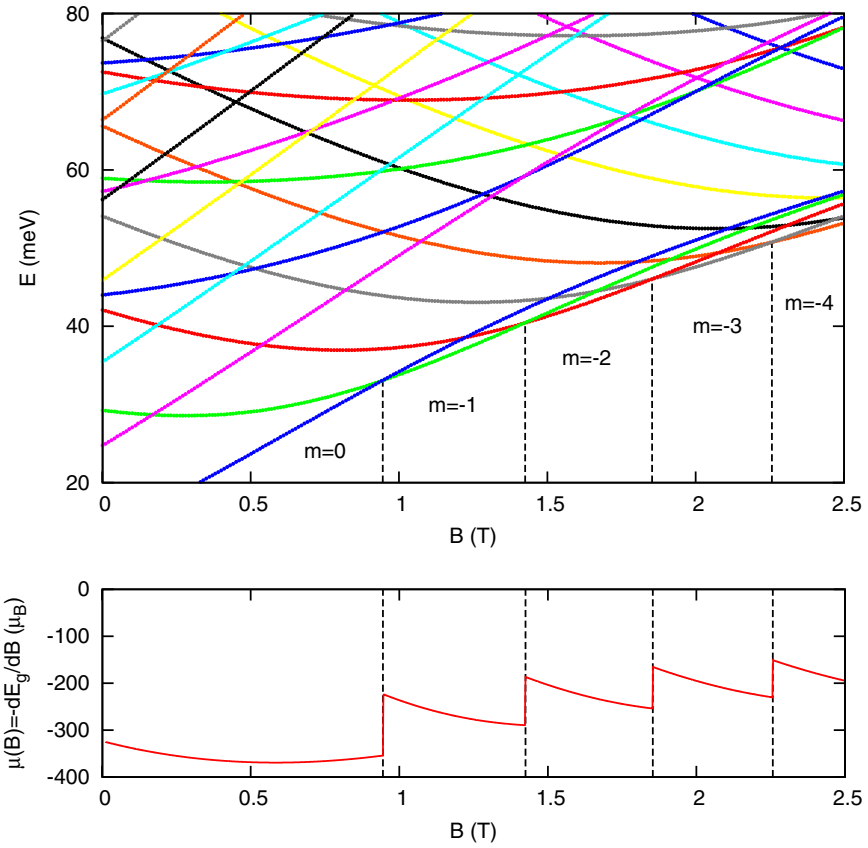

FIG. 2. (top) Energy levels for the ground and first excited states (in meV) as a function of the magnetic field strength B (in T) for a graphene quantum dot with $R = 70$ nm. The magnetic field phase transition (critical) values $B_{PT} \simeq 0.945$, 1.423, 1.852, 2.256, ... T are indicated by vertical dashed lines leading an infinite sequence of critical points with different m with $m = 0, -1, -2, -3, \ldots$ (bottom) Magnetic moment (in μ_B units) of the graphene quantum dot as a function of the applied magnetic field. The discontinuities are indicated by vertical dashed lines at the above critical points.

Let us investigate now the ground state energy of the system E_g (the lowest positive energy) as a function of the magnetic field strength for $\tau = 1$. Its value changes from $E = 13.6$ meV for $B = 0$ to the lowest Landau level $E_{LL0} = v_F\sqrt{2e\hbar B}$ when $B \to \infty$. As the magnetic field increases, there is a sequence of phase transitions (critical) points which appear at $B_{PT} \simeq 0.945$, 1.423, 1.852, 2.256, ... (in T) whose quantum numbers m are decreasing following the sequence $m = 0, -1, -2, -3, \ldots$, (Fig. 2 (top)) and as a consequence the ground state parity is alternately changing. We can calculate the magnetic moment of the electron $\mu(B) = -\frac{dE_g}{dB}$ (see, e. g.[29]) whose behavior is depicted in Fig. 2 (bottom) for 0.5 T $\leq B \leq$ 4 T. This type of PT is a well known feature of electrons in a magnetic field in a confinement potential, see for instance[29,30] and references therein. It is noticeable the appearance of discontinuities of $\mu(B)$ at the particular magnetic field values B_{PT} where the ground state energy is not analytical, which is a crucial signature of PT. Furthermore, in order to characterize these ground state energy PT we have studied the behavior of the energy gap $\Delta E \equiv |E_1 - E_g|$ near to the critical points and we have found that $\Delta E \sim |B - B_{PT}|^{z\nu}$ with $z\nu = 1$ as it is shown in Fig. 3.

We have also investigated the connection between the evolution of a wave-packet for a particular election of its initial shape and the phase transition point. For this purpose, we have constructed the wave-packet as a superposition of eigenstates choosing a Gaussian distribution population of the energy levels around the ground state positive energy

$$\psi(\mathbf{r}) = \sum_{n=0}^{\infty}\sum_{m=-\infty}^{\infty} c_{n,m}\psi_{(n,m)}(\mathbf{r}) \tag{3}$$

All article content, except where otherwise noted, is licensed under a Creative Commons Attribution 3.0 Unported license. See: http://creativecommons.org/licenses/by/3.0/
Downloaded to IP: 150.214.23.191 On: Wed, 18 Jun 2014 09:04:25

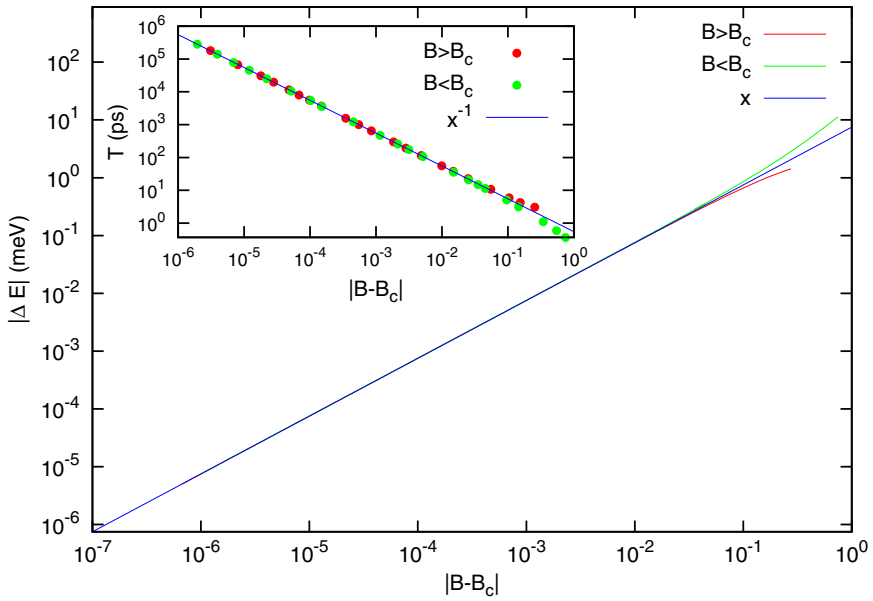

FIG. 3. (Main graph) Scaling of the energy gap $\Delta E \equiv |E_1 - E_g|$ around the PT point $B_{PT} \simeq 0.945$ T which shows a dependence $\Delta E \sim |B - B_{PT}|^{-1}$. (Inset) Divergence of the oscillations period near the same critical point. For each value of B the period T (symbols) has been computed, from the autocorrelation function of a Gaussian wave-packet centered around the two first energy levels. with $\sigma \sim 1.7$.

$c_{n,m} = ce^{-(m-m_0)^2/2\sigma^2} e^{-(n-n_0)^2/2\sigma^2}$ and with c such that $\sum_{n=0}^{\infty} \sum_{m=-\infty}^{\infty} |c_{n,m}|^2 = 1$. We have studied the wave-packet dynamic of this initial wave-packet for different values of the intensity of the magnetic field B. To analyze the evolution of the wave-packet we used the autocorrelation function defined as $A(t) = \int \psi^*(\mathbf{r}, 0)\psi(\mathbf{r}, t)d\mathbf{r}$. An alternative approach based on uncertainty information entropies relations has been also proposed.[31] The wave-packet regeneration then occurs when $|A(t)|^2$ approximatively returns to its initial value of unity.

We have calculated the time evolution of the autocorrelation function for an initial wave-packet centered around the ground state with width σ and for $R = 70$ nm for different values of the magnetic field B. We have found that for B around the critical values B_{PT} the wave-packet has a oscillation pattern with a period that is increasing when B is approaching B_{PT}. The time dependence of the autocorrelation function is illustrated if Fig. 4 for $B = 0.9$ T $< B_{PT}$ and $B = 1.0$ T $> B_{PT}$, respectively. Clearly the autocorrelation function returns to the value of unity oscillating with a period $T_B = 11.49$ ps for $B = 0.9$ T and $T_B = 10.79$ ps for $B = 1.0$ T. On the other hand, $T_B \sim |B - B_{PT}|^{-\theta}$ for $B \sim B_{PT}$ with scaling parameter $\theta = 1$. This behavior is clearly shown in Fig. 3 where T_B is displayed as a function of B in a log-log scale for magnetic field strengths around the PT point $B_{PT} \simeq 0.945$ T. From the slope of a straight-line fit one easily finds $\theta = 1$. Additionally, when $B < B_{PT}$ the wave-packet describes a main clockwise rotation and a forward and backward pulsating movement superimposed to the above one (Fig. 4 (top)). After the PT point $B > B_{PT}$ the wave-packet has an analogous motion but the main rotating movement is counter clockwise (Fig. 4 (bottom)). On the other hand, the wave-packet doesn't rotate at the PT point - in fact it takes an infinite time to do so - and only the forward and backward pulsating motion remains (Fig. 4 (middle)). For other values of B far from the critical points the temporal evolution of the wave-packets doesn't have this oscillation pattern.

The wave-packet behavior is also clearly illustrated in Fig. 5 (top) where we have shown simultaneously the temporal evolution of $|A(t)|^2$ at different values of 0.5 T $< B <$ 2.5 T. The wave-packet has been created with $\sigma = 1$. We observe how the periods of motion diverge at the ground state energy critical points $B_{PT} \simeq 0.945, 1.423, 1.852, 2.256$ and we have checked that this behavior remains for different values of σ.

All article content, except where otherwise noted, is licensed under a Creative Commons Attribution 3.0 Unported license. See: http://creativecommons.org/licenses/by/3.0/
Downloaded to IP: 150.214.23.191 On: Wed, 18 Jun 2014 09:04:25

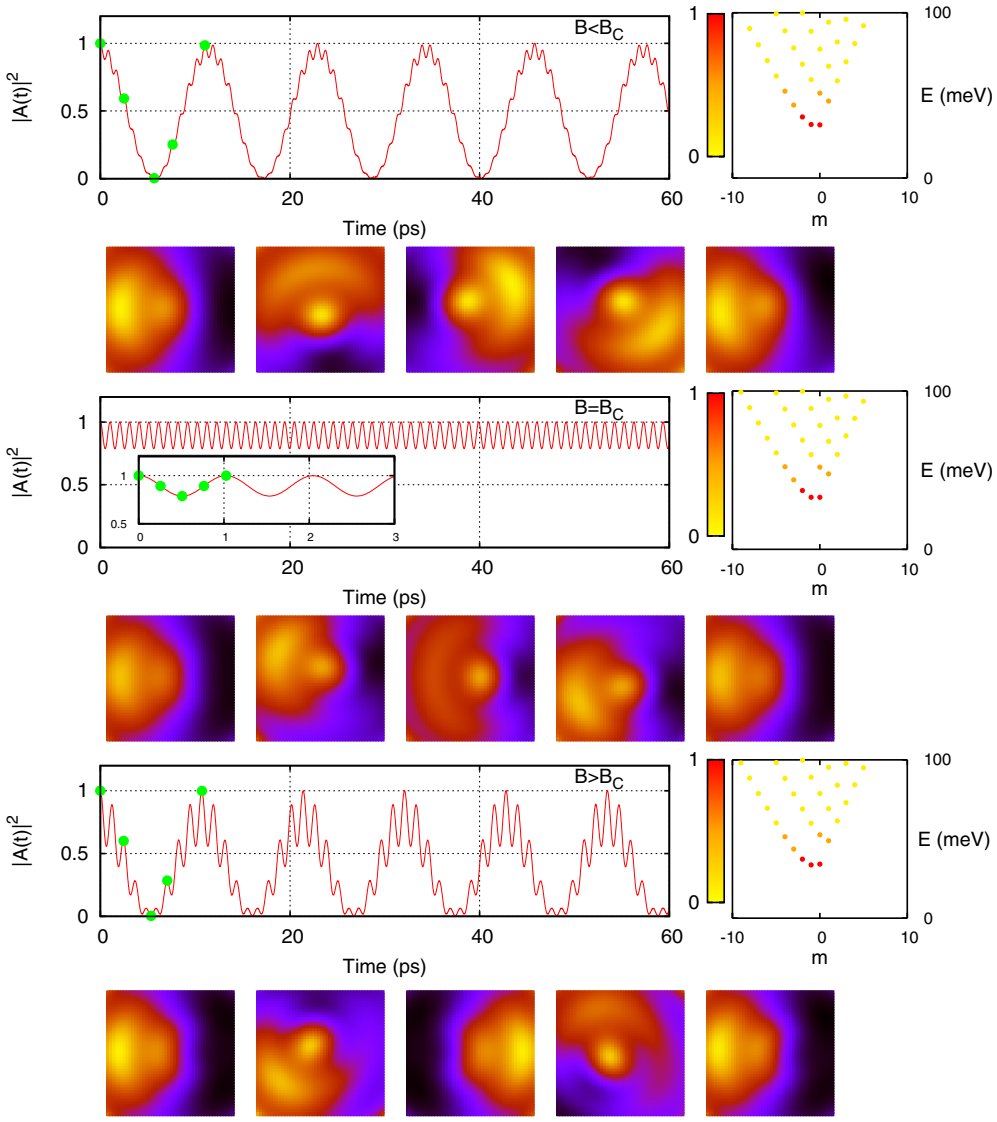

FIG. 4. Time dependence of the autocorrelation function, for an initial Gaussian wave-packet with $\sigma = 2$, near the first critical point, snapshots of the density function $|\psi(\mathbf{r})|^2$ evolution at the green points and level energy panel with level population, from red (high probability) to yellow (low probability) color scale, just before the critical point (top panels), in the critical point (middle panels) and after the critical point (bottom panels).

To confirm the robustness of the results above, we have also calculated the total entropy of the temporal evolution of the autocorrelation function

$$S = -\frac{1}{T_{max}} \int_0^{T_{max}} |A(t)|^2 \ln |A(t)|^2 dt, \tag{4}$$

which we have numerically computed for 0.5 T $< B <$ 2.5 T and for $T_{max} = 100$ ps great enough to capture all the wave-packet dynamic for different magnetic field strengths. It is apparent from Fig. 5 (bottom) that the entropy has maxima at the critical points where the autocorrelation function is quasi-constant.

All article content, except where otherwise noted, is licensed under a Creative Commons Attribution 3.0 Unported license. See: http://creativecommons.org/licenses/by/3.0/
Downloaded to IP: 150.214.23.191 On: Wed, 18 Jun 2014 09:04:25

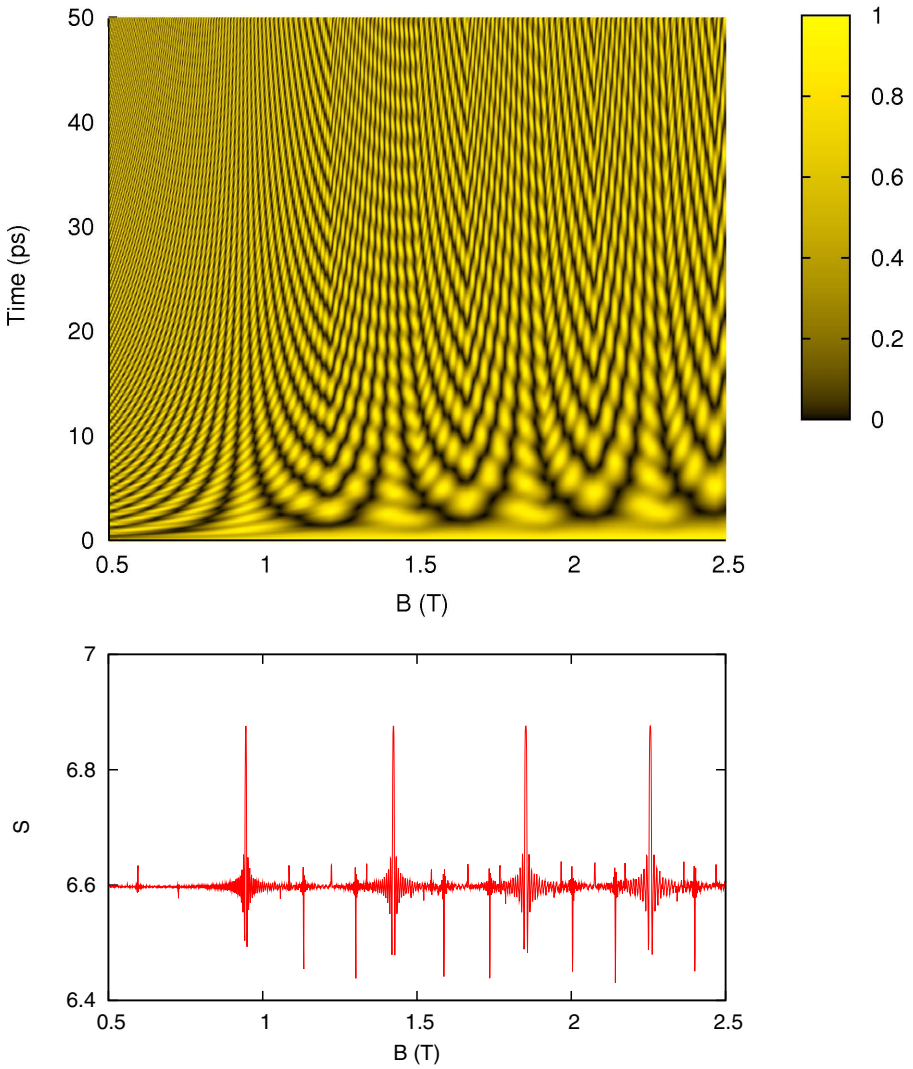

FIG. 5. (Top) Time dependence of the autocorrelation function for an initial Gaussian wave-packet with $\sigma = 1$ for all values of B which shows that when B is around the different critical values $B_{PT} \simeq 0.945, 1.423, 1.852, 2.256, \ldots$, the oscillation periods are increasing when B is approaching B_{PT}. (Bottom) Total entropy S of the temporal evolution of the autocorrelation function for the above initial wave-packets as a function of the magnetic field. The entropy shows very sharp maxima at magnetic field values B_{PT} where the PTs occur.

III. DIRAC OSCILLATOR MODEL

As a second system under study to prove the generality of our findings above and to check the ground state energy PT characterization, we have considered the case of a fermionic relativistic harmonic oscillator when an additional constant magnetic field is applied. This relativistic fermion has mass m and charge $-e$. The relativistic fermion is described by the following Hamiltonian:

$$H = c\boldsymbol{\alpha} \cdot (\mathbf{p} - im\beta\omega\mathbf{r} + e\mathbf{A}) + \beta mc^2 \tag{5}$$

where ω is the Dirac oscillator frequency, c the speed of light and β and $\boldsymbol{\alpha}$ the usual Dirac matrices. We performed our study in the axial gauge where a constant magnetic field $\mathbf{B} = B\vec{e}_z$ is described by the vector potential $\mathbf{A} \equiv \frac{B}{2}(-y, x, 0)$, and the cyclotron frequency is given by $\omega_c \equiv \frac{eB}{m}$. Introducing

All article content, except where otherwise noted, is licensed under a Creative Commons Attribution 3.0 Unported license. See: http://creativecommons.org/licenses/by/3.0/
Downloaded to IP: 150.214.23.191 On: Wed, 18 Jun 2014 09:04:25

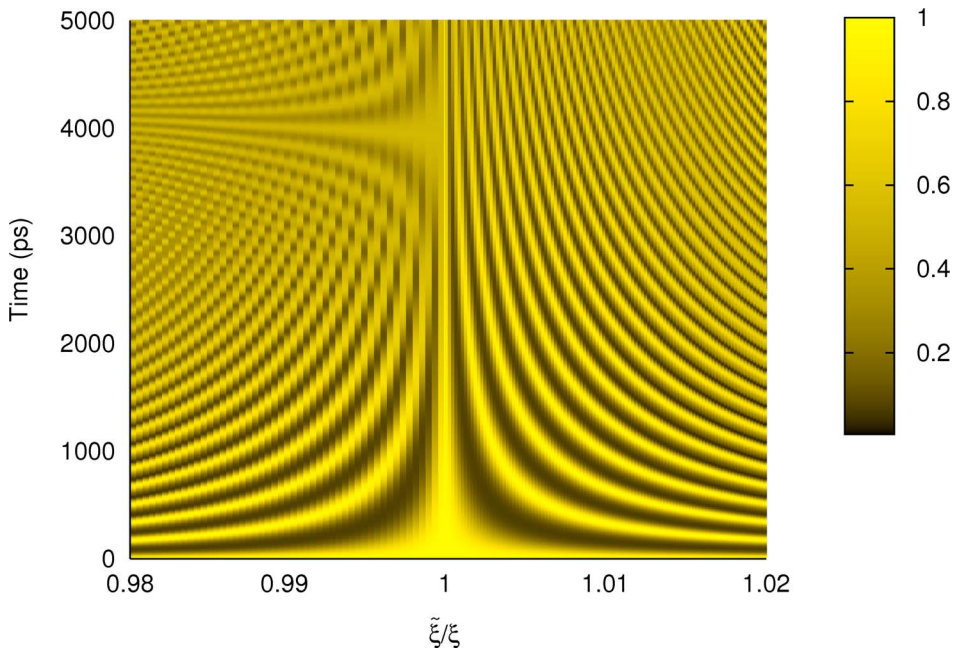

FIG. 6. Time dependence of the autocorrelation function for an initial Gaussian wave-packet with $\sigma = 1$ for several values of the relative coupling strengths $\tilde{\xi}/\xi$ which shows that the oscillation periods are increasing when $\tilde{\xi}/\xi$ is approaching 1.

the quantities

$$\tilde{\omega} \equiv \omega_c/2, \qquad \xi \equiv \hbar\omega/mc^2 \qquad \tilde{\xi} \equiv \hbar\tilde{\omega}/mc^2 \tag{6}$$

$$\mu = \frac{1}{2}\left(\frac{\tilde{\omega}}{\omega} - \frac{\omega}{\tilde{\omega}}\right) \tag{7}$$

the eigenergies are given[32] by

$$E_n = \pm mc^2\sqrt{1 + 2(\xi - \tilde{\xi} - 2\mu(\xi\tilde{\xi})^{1/2})(n+1)}, \tag{8}$$

for $n = 1, 2, \ldots$ and

$$E_0 = \pm mc^2 \tag{9}$$

in the case $\tilde{\xi} < \xi$ and by

$$E_n = \pm mc^2\sqrt{1 + 2(\tilde{\xi} - \xi + 2\mu(\xi\tilde{\xi})^{1/2})(n+1)}, \tag{10}$$

for $n = 0, 1, 2, \ldots$ in the case $\tilde{\xi} > \xi$. It has been proof[32] that this system exhibits a PT for a critical coupling $\left(\tilde{\xi}/\xi\right)_c = 1$ and that there is[32] an universal scaling law for the energy gap $\Delta E \to 0$ when $\left|\frac{\tilde{\xi}}{\xi} - \left(\frac{\tilde{\xi}}{\xi}\right)_c\right| \to 0$ with scaling exponent 1, that is, $\Delta E \sim \left|\frac{\tilde{\xi}}{\xi} - \left(\frac{\tilde{\xi}}{\xi}\right)_c\right|$.

Next, we have constructed the wave-packet as in Eq. (3), that is, choosing a Gaussian distribution population of the energy levels around the ground state positive level. We find the same behavior in the PT point than in the case of the graphene quantum dot as it can be depicted in the carpet in Figure 6.

IV. SUMMARY

Summing up, in this work we have provided a new tool to visualize and characterize phase transitions in terms of wave-packet dynamics using as illustrative systems a graphene quantum dot

All article content, except where otherwise noted, is licensed under a Creative Commons Attribution 3.0 Unported license. See: http://creativecommons.org/licenses/by/3.0/
Downloaded to IP: 150.214.23.191 On: Wed, 18 Jun 2014 09:04:25

in a perpendicular magnetic field model and a Dirac oscillator in a magnetic field. We have shown that the autocorrelation function shows that above and below each critical point the wave-packet has oscillations whose period diverges at the PT point in both models. Furthermore, the Shannon entropy of the square of the autocorrelation function shows relative maxima at the critical points which reveals it as a very suitable PT indicator.

ACKNOWLEDGMENTS

This work was supported by Spanish MICINN projects FIS2011-24149 and FIS2009-08451, CEI BioTic UGR project 20F12.41 and Junta de Andalucia projects FQM-165/0207 and FQM219.

[1] J. H. Eberly, N. B. Narozhny, and J. J. Sánchez-Mondragón, Phys. Rev. Lett. **44**, 1323 (1980).
[2] I. Sh. Averbukh and J. F. Perelman, Phys. Lett. A **139**, 449 (1989); Acta Phys. Pol. A **78**, 33 (1990).
[3] D. L. Aronstein and C. R. Stroud, Jr., Phys. Rev. A **55**, 4526 (1997).
[4] R. W. Robinett, Phys. Rep. **392**, 1 (2004).
[5] J. A. Yeazell, M. Mallalieu, and C. R. Stroud, Jr., Phys. Rev. Lett. **64**, 2007 (1990).
[6] G. Rempe, H. Walther, and N. Klein, Phys. Rev. Lett. **58**, 353 (1987); T. Baumert *et al.*, Chem. Phys. Lett. **191**, 639 (1992); M. J. J. Vrakking, D. M. Villeneuve, and A. Stolow, Phys. Rev. A **54**, R37-R40 (1996); A. Rudenko *et al.*, Chem. Phys. **329**, 193 (2006).
[7] E. Romera and F. de los Santos, Phys. Rev. B **80**, 165416 (2009).
[8] V. Krueckl and T. Kramer, New J. Phys. **11**, 093010 (2009).
[9] J. J. Torres, E. Romera, Phys. Rev. B **82**, 155419 (2010).
[10] E. Romera, Phys. Rev. A **84**, 052102 (2011).
[11] A. Prástaro, Nonl. Anal. Real World Appl. **13**, 2491 (2012).
[12] E. Romera and A. Nagy, Phys. Lett. A **375**, 3066 (2011).
[13] E. Romera, K. Sen and A. Nagy, J. Stat. Mech., P09016 (2011).
[14] E. Romera, M. Calixto, and A. Nagy, EPL **97**, 20011 (2012).
[15] A. Nagy and E. Romera, Physica A, doi:10.1016/j.physa.2012.02.024.
[16] M. Calixto, A. Nagy, I. Paradela and E. Romera, Phys. Rev. A **85**, 053813 (2012).
[17] A. H. Castro Neto, F. Guinea, N. M. R. Peres, K. S. Novoselov and A. K. Geim, Rev. Mod. Phys. **81**, 109–162 (2009).
[18] A. K. Geim, Science **324**, 1530 (2009).
[19] K. S. Novoselov Phys. World **22**(8), 27 (2009).
[20] C. Lee, X. Wei, J. W. Kysar, and J. Hone, Science **321**, 385 (2008); A. A. Balandin *et al.*, Nano Lett. **8**, 902 (2008).
[21] J. H. Chen, C. Jang, S. Xiao, M. Ishigami, and M. S. Fuhrer, Nature Nanotech. **3**, 206 (2008).
[22] N. N. Klimov *et al.*, Science **336**, 1557 (2012).
[23] L. Ponomarenko, F. Schedin, M. Katsnelson, R. Yang, E. Hill, K. Novoselov and A. Geim, Science **320**, 356 (2008).
[24] S. Schnez, F. Molitor, C. Tampfer, J. Güttinger, I. Shorubalko, T. Ihn, and K. Ensslin, Appl. Phys. Lett. **94**, 012107 (2009).
[25] P. Recher and B. Trauzettel, Nanotechnology **21**, 302001 (2010).
[26] T. Müller, J. Güttinger, D. Bischoff, S. Hellmüller, K. Ensslin, and T. Ihn, Appl. Phys. Lett. **101**, 012104 (2012).
[27] S. Schnez, K. Ensslin, M. Sigrist, and T. Ihn, Phys. Rev. B **78**, 195427 (2008).
[28] M. V. Berry and R. J. Mondragon, Proc. R. Soc. London, Ser. A **412**, 53 (1987).
[29] M. Wagner, U. Merkt and A. V. Chaplik, Phys. Rev. B **45**, 1951 (1992).
[30] S. M. Reimann, M. Manninen, Rev. Mod. Phys. **74**, 1283 (2002).
[31] E. Romera, and F. de los Santos, Phys. Rev. Lett. **99**, 263601 (2007); Phys. Rev. A **78**, 013837 (2008).
[32] A. Bermudez, M. A. Martín-Delgado, and A. Luis, Phys. Rev. A **77**, 063815 (2008).

All article content, except where otherwise noted, is licensed under a Creative Commons Attribution 3.0 Unported license. See: http://creativecommons.org/licenses/by/3.0/
Downloaded to IP: 150.214.23.191 On: Wed, 18 Jun 2014 09:04:25